Radiation reaction of electrons at laser intensities up to 10^{25} W/cm^2

Xilin Zhou

Webster Schroeder High School

Advisor: *Dr. S. X. Hu*

Laboratory for Laser Energetics

University of Rochester

Rochester, New York

November 2015

Abstract

Recent developments in high-power laser technology allowing for laser intensities from 10^{22} W/cm^2 up to 10^{24} W/cm^2 have opened up the study of the super-intense laser acceleration of electrons to tens of GeV energies. These intensities may be attainable in the next generation of super-powerful lasers such as EP-OPAL, a proposed extension of the Laboratory for Laser Energetics OMEGA EP Laser System which can potentially reach laser intensities as high as 10^{24} W/cm^2. Previous work on this subject did not account for the radiation reaction force, which is the recoil force caused by the electromagnetic radiation emitted by an accelerating charged particle. In this work, two possible scenarios (an electron originally bound in a highly charged ion, and a counter-propagating 1-GeV electron pulse) were tested. The first scenario, involving the highly charged ion, showed little difference between simulations with and without the radiation reaction force. However, the second scenario, involving the counter-propagating 1-GeV electron pulse, showed the electrons losing significant amounts of energy when the radiation reaction force was accounted for. If harnessed, this radiated energy could be applied in medical and other research fields. Future studies will look into the spectrum and power of the radiated energy.

I. Introduction

Technological advances over the past two decades have made laser intensities of 10^{22} W/cm^2 obtainable [1]. It may be possible to have laser intensities as high as 10^{24} W/cm^2 in the near future [2]. The laser field strengths at these laser intensities are about three to four orders of magnitude greater than the Coulomb field that binds the ground-state electron in atomic hydrogen. These high laser intensities have opened up the study of the super-intense laser acceleration of electrons. At these super-high intensity levels, electrons accelerated to ultrarelativistic velocities may strongly radiate while their velocity changes. Due to momentum conservation, these electrons experience the radiation reaction (RR) force, which is the force caused by the radiation emitted from the accelerating electron. The radiation released from the electron is directed predominantly along the direction of the particle's motion, within a small range of angles. As a result, the electron trajectory when travelling at relativistic velocities can be significantly changed, leading to changes in the final electron energies as well.

When a free electron is accelerated directly by the laser field, it is expelled from the laser focus region before the laser pulse has reached its maximum intensity. Once expelled, the electron no longer experiences any laser fields. Therefore, even with super-intense lasers, the electrons only acquire a few hundred MeV of energy [3]. The same difficulties are inherent to the alternative method of laser acceleration of electrons initially bound in neutral targets. The electrons are "born" prematurely due to the lower intensities of the increasing laser field, and do not experience the peak intensity of the laser field. This results in final electron energies well below the GeV energies expected from currently available laser intensities [4].

A scenario wherein electrons ionized from highly charged ions interacting with an intense laser field has been proposed as a method for the super-intense laser acceleration of electrons [5,

6]. The ion species are chosen depending on the laser intensity to ensure that the highly charged ions are only ionized when the laser field approaches its peak intensity. The results showed that the ionized electrons are then accelerated by the intense laser field to nearly the speed of light and gain significant amounts of energy while surfing on the laser pulse. However, these previous calculations did not consider how the radiation reaction affects the electron acceleration in such a scenario.

In order to further understand the effects of the radiation reaction force at relativistic velocities, we also consider another scenario in which a 1-GeV electron pulse counter-propagates with respect to the laser pulse. The point of contact between the laser pulse and the electron pulse is at the center of the laser focus. Since the electron pulse and the laser pulse are initially moving towards each other, the electron pulse's deceleration due to the tightly focused laser field is great. Therefore, the radiation reaction force could be significant, which may result in highly modified electron trajectories in such a head-on collision.

In this paper, we analyze the effects of the radiation reaction force on the electron trajectories and final energies for the two scenarios involving the electron originally bound in a highly charged ion, and the counter-propagating electron pulse. We assume the laser pulse is linearly polarized and propagating along the z axis. Our simulations use lasers expected to become available in the near future. The fields of these lasers can be focused to a small area, thus achieving intensities of up to the order of 10^{24} W/cm^2 in the laser focus region. The relativistic Monte Carlo method is applied to simulate the laser acceleration of electrons in hydrogen-like highly charged ions (HCI), and the interactions between the laser pulse and the counter-propagating electron pulse. For each laser intensity studied, the pulse waist (radius at laser focus) is 10 μm. Our principal result is the demonstration that the final energies and ejection angles of

the ionized electron are not greatly affected by the radiation reaction force for the HCI case, whereas the final energies and electron angles for the head-on collision between the electron pulse and the super-intense laser pulse case are significantly altered by the radiation reaction force.

The paper is organized as follows. In **Sec. II**, we outline the classical relativistic Monte Carlo approach used in our simulations as well as the preparation of the ensemble of initial conditions. In **Sec. III**, we present the results of our numerical simulations and explain the major features of our simulation results. Finally, in **Sec. IV**, we summarize our results and present our conclusions.

II. Simulation Methods

A. Relativistic classical trajectory Monte Carlo method

The classical relativistic approach for solving the relativistic Newton's equation of motion is capable of treating the Coulomb potential and the laser-focusing effects three-dimensionally. Although the method cannot simulate the quantum ionization process in the highly charged ion scenario, it can describe the interaction of both an ionized electron and an electron pulse with the laser field with quantitative accuracy.

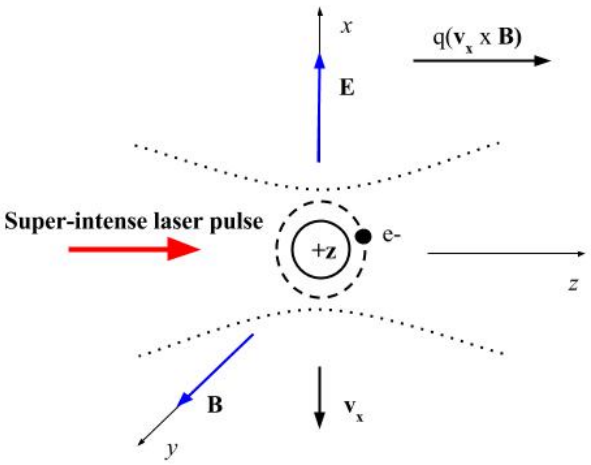

Figure 1: Schematic diagram of the interaction of an intense laser pulse with a hydrogen-like, highly charged ion that results in ionization of its electron. The laser pulse propagates along the *z* axis while the major electric field *E* and the magnetic field *B* of the laser pulse are linearly polarized along the *x* and *y* axes respectively. The vector $\mathbf{v_x}$ indicates the component of the electron velocity along the *x* axis, and *e-* indicates the electron charge. The Lorentz force is represented in the upper right of the figure by $q(\mathbf{v_x} \times \mathbf{B})$.

We first consider the interaction of an ultra-intense laser pulse with a hydrogen-like, highly charged ion. *Fig. 1* shows the interaction scheme. The laser pulse is assumed to be linearly polarized along the *x* axis and to propagate along the *z* axis; it is focused to a small spot having a radius (or beam waist w_0) on the order of 10 μm. For such a tightly focused laser beam, the fifth-order expansion of the Maxwell equation has been used to describe the complicated laser field components. As was shown in reference [6], such a description of laser fields is necessary for tight focusing.

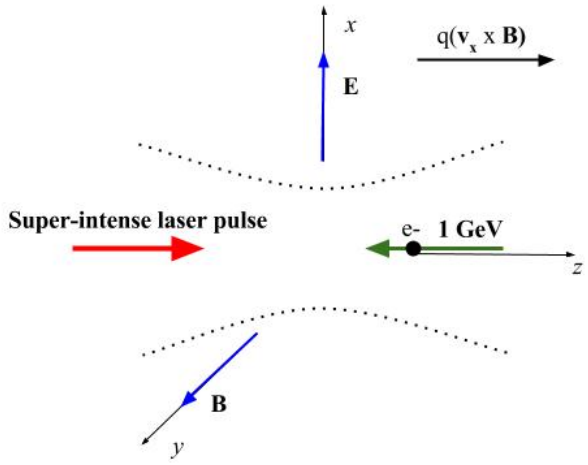

Figure 2: Schematic diagram of the interaction of an intense laser pulse with a 1-GeV counter-propagating electron pulse. The directions and indicators of the various vectors are equivalent to those described in *Fig. 1*.

The second scenario we consider is the interaction of an ultra-intense laser pulse with a 1-GeV counter-propagating electron pulse, which is schematically illustrated in *Fig. 2*. The laser pulse is assumed to have the same properties described in *Fig. 1*.

When taking into consideration the RR force, the motion of the ionized electron and the electron pulse in both an electromagnetic field and a Coulomb field is described by

$$\frac{d\boldsymbol{p}}{dt} = -e\left(\boldsymbol{E}_L + \boldsymbol{E}_C + \frac{\boldsymbol{p}\times\boldsymbol{B}_L}{m_e\gamma c}\right) + \boldsymbol{F}_{RR}, \qquad (1)$$

where the RR force takes the Landau-Lifshitz [7] format, i.e.,

$$\boldsymbol{F}_{RR} \approx -\left(\frac{2e^4}{3m_e c^5}\right)\gamma^2\boldsymbol{v}\left[\left(\boldsymbol{E} + \boldsymbol{v}\times\frac{\boldsymbol{B}}{c}\right)^2 - \frac{(\boldsymbol{E}\cdot\boldsymbol{v})^2}{c^2}\right], \qquad (2)$$

and $\gamma = \sqrt{1 + \left(\frac{p}{m_e c}\right)^2}$ is the Lorentz relativistic factor; c is the speed of light in vacuum; **r** and **p** are the coordinate and mechanical momentum vectors of the electron, respectively; $\mathbf{E}_L$ is the laser electric field; and $\mathbf{E}_c$ is the Coulomb field of the ion in the HCI case, which is absent in the

electron pulse scenario. The above vector equation can also be written in terms of its three components,

$$dp_x/dt = -e\left[E_{L_x} + E_{C_x} + \left(p_y B_{L_z} - p_z B_{L_y}\right)/(\gamma c)\right] + F_{RR_x},$$

$$dp_y/dt = -e\left[E_{L_y} + E_{C_y} + \left(p_z B_{L_x} - p_x B_{L_z}\right)/(\gamma c)\right] + F_{RR_y}, \quad (3)$$

$$dp_z/dt = -e\left[E_{L_z} + E_{C_z} + \left(p_x B_{L_y} - p_y B_{L_x}\right)/(\gamma c)\right] + F_{RR_z},$$

where the three components of the radiation reaction force can be written as,

$$F_{RR_x} = G(D - M)v_x,$$

$$F_{RR_y} = G(D - M)v_y, \quad (4)$$

$$F_{RR_z} = G(D - M)v_z,$$

where the quantities are $G = -\left(\frac{2e^4}{3m_e c^7}\right)\gamma^2$; $D = \left(cE_x + v_y B_z - v_z B_y\right)^2 + \left(cE_y + v_x B_z + v_z B_x\right)^2 + \left(cE_z + v_x B_y - v_y B_x\right)^2$; and $M = \left(E_x v_x + E_y v_y + E_z v_z\right)$. The three components of the velocity vector **v** are equal to $v_x = p_x/m_e\gamma,\ v_y = p_y/m_e\gamma,\ v_z = p_z/m_e\gamma$.

Using the Runge-Kutta method with variable step size, we numerically integrate *Eqs. (1)* for each classical electron trajectory. For the highly charged ion scenario, the electron trajectories are randomly chosen from a prepared relativistic microcanonical ensemble, which mimics the electronic ground state of the target. The electron ionization time is calculated by the over-the-barrier model [6], in which the electron gets free at the time when the laser field suppresses the Coulomb barrier below the ground-state energy level. For the counter-propagating electron pulse scenario, the initial momentum of the pulse along the *z* axis is randomly chosen from a normally distributed set of initial momenta. Our results are presented in **Sec. III** as plots of the normalized count of electrons as a function of the emission angle, and plots of the normalized count of electrons as a function of the electron's final-state energy.

B. Preparation of electron pulse scenario

In the electron pulse scenario, an initial set of parameters is needed for each trajectory. Therefore, we prepared a normally distributed ensemble of size 200,000 of initial momenta along the *z* axis of the electron pulse, and calculated the initial position of the electron pulse along the *z* axis. To prepare the previously described ensemble, we first calculate the mean p_z that the normally distributed ensemble will be centered around. The momentum of a relativistic particle can be described as,

$$p_{z_0} = m_e c\sqrt{\gamma^2 - 1}\,, \qquad (5)$$

where $\gamma = (E/m_e c^2) + 1$ with $E = m_e\gamma c^2 - m_e c^2$. The momentum p_{z_0} is negative, indicating that the electron is moving towards the negative *z* axis (head-on collision with the laser pulse in *Fig. 2*). We then consider the function of the normal distribution to be written as,

$$f(p_z) = \frac{1}{\sigma\sqrt{2\pi}} \exp\left(-\frac{(p_z - p_{z_0})^2}{2\sigma^2}\right), \qquad (6)$$

where σ is the standard deviation. We assume a 2% momentum spread [i.e., the full width at half maximum $FWHM = 2\sqrt{2ln2}\sigma$ is 2% of p_{z_0}]. With this distribution function, we assign the value of p_z to each of the total 200,000 electrons. The initial momenta of the electron pulse along the *x* and *y* axes are assumed to be 0. The electron pulse is initially positioned so that it reaches the center of the laser focus at time $t = 0$ (at the peak of laser intensity). Since the scenario is modeled with a start time of t_0 = -20 fs, the initial position of the electron pulse along the *z* axis can be written as, $z = p_z \cdot t_0/m_e\gamma$. The initial position of the electron pulse along the *x* and *y* axes is assumed to be 0 in single-trajectory simulations, while for ensemble simulations the electron pulse has the same cross-section as the laser pulse in the *x*-*y* plane.

III. Results and Discussion

Using the three-dimensional Monte Carlo simulations described in the previous section, we investigated the RR effects of electrons exposed to laser pulses of different intensities. In our simulations, the laser wavelength is equal to λ=910 nm, which can be generated by the optical parametric chirp-pulse-amplification (OPCPA) technique [8]. The laser pulse has a Gaussian temporal shape with a full-width at half-maximum (FWHM) of 20 fs and is focused to a beam waist w_0=10 μm.

A. Highly charged ions as targets

In this section, we show the simulation results with and without radiation reaction for electrons from highly charged ions interacting with an intense laser beam having various intensities. We find that the final energies and electron angles are only slightly affected by the RR force even at intensities above 10^{24} W/cm^2. We also present qualitative explanations for the physics behind our results.

The idea of the highly charged ion for laser acceleration of electrons is to allow the electron to remain at the laser focus until the laser pulse reaches the maximum intensity. At that point, the electron is ionized and continues to experience the maximum laser intensity, therefore being accelerated to GeV energies. This requires that the ion target is matched to the maximum laser intensity so that little ionization occurs during the rise time of the laser pulse, but significant ionization through "over-the-barrier" mechanisms occurs at the peak laser intensity. Therefore, in our calculations, we selected charges of the ion target that corresponded with the intensity of the laser pulse. The charges of the ion target at laser intensities 10^{24} and 10^{25} W/cm^2 are z = +43.0 and z = +64.0, respectively for Tc^{42+} ions and Gd^{63+} ions.

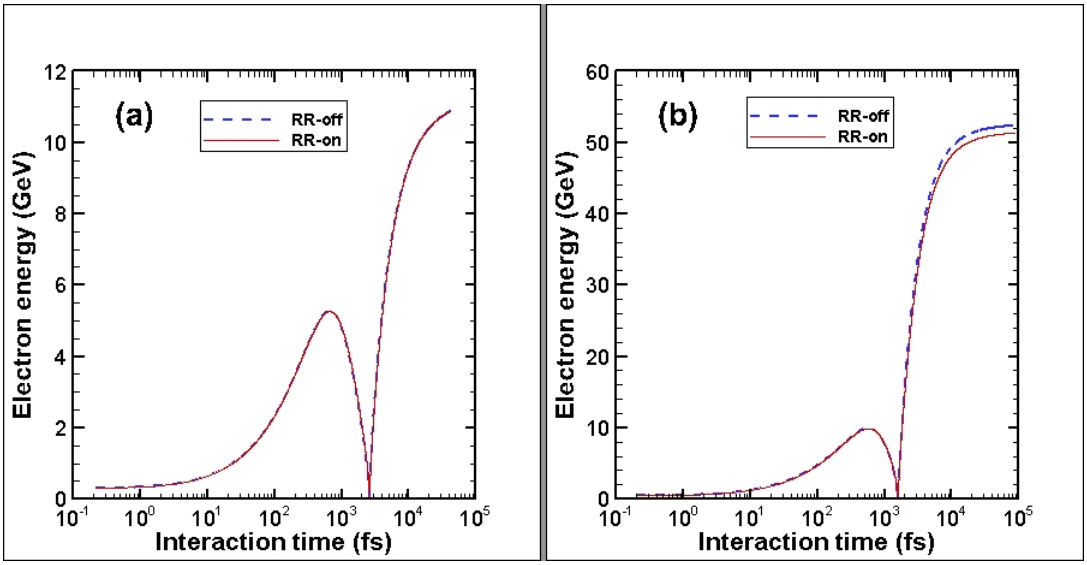

Figure 3: Monte Carlo simulation results for single highly charged ion of (a) Tc^{42+} and (b) Gd^{63+} interacting with a 10^{24} W/cm^2 and 10^{25} W/cm^2 laser, respectively.

We conducted single trajectory simulations with and without the RR effects. The HCI of Tc^{42+} and Gd^{63+} were initially placed at the center of the laser focus. The kinetic energy of the electron during the trajectory was calculated by $E = (\gamma - 1)m_e c^2$. We plot the electron energy as a function of interaction time in Figure 3. The plot shows that there is very little difference in the final electron energies between radiation reaction on and off. Since the electron is highly relativistic and is "surfing" on (co-moving with) the laser wave, the interaction time in the laboratory frame is much longer than the laser pulse duration (20 fs). In the interactions of the 10^{24} W/cm^2 intensity laser with Tc^{42+} ions, the final difference between trajectories with radiation reaction on and off is less than 0.01 GeV. This value is insignificant in comparison with the final electron energies of ~11 GeV. At a laser intensity of 10^{25} W/cm^2, the final difference between trajectories is approximately 1.3 GeV, which is only ~2% of the final electron energy of ~51 GeV. The final energy for the RR-on case is only slightly lower than that for the RR-off case [see *Fig. 3(b)*].

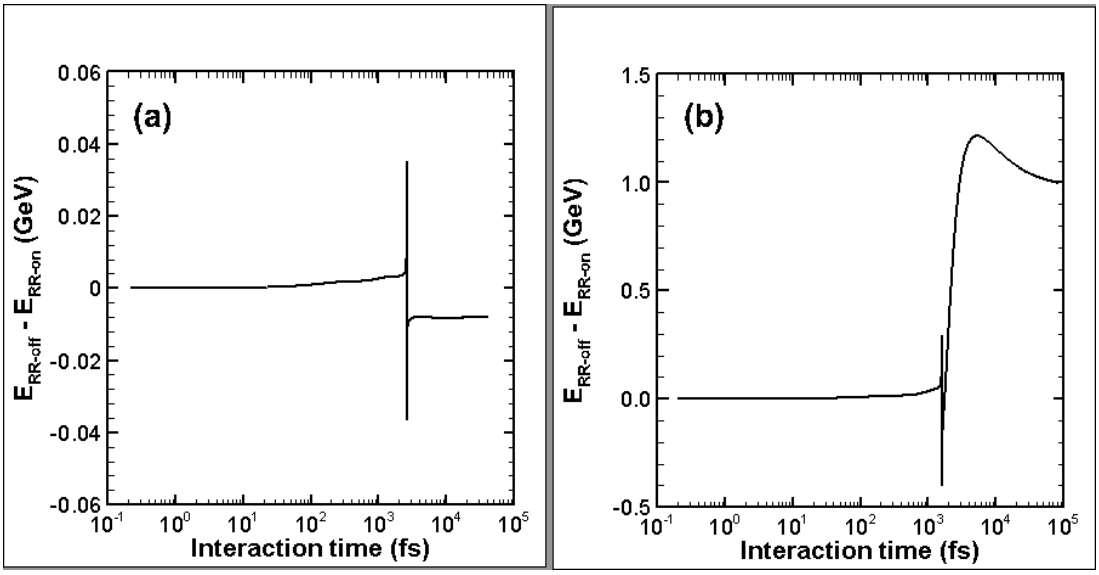

Figure 4: The energy difference in GeV between simulations with and without RR for the cases shown in *Fig. 3* plotted as a function of time in fs. (a) The ionized electron is interacting with a 10^{24} W/cm^2 laser pulse. (b) The ionized electron is interacting with a 10^{25} W/cm^2 laser pulse.

To further understand the RR effects of the laser-electron acceleration from HCI, we plot the energy difference in *Fig. 4* for the two cases discussed in *Fig. 3*. We see that the energy difference between RR-on and RR-off remains near zero for the first 1000 fs. Although the initial acceleration after ionization due to the peak-intensity laser field is large, the magnitude of the acceleration is not great enough for any noticeable energy differences due to radiation reaction. However, we see that the radiation reaction effects suddenly show up at $t \approx 2500$ fs in *Fig. 4(a)* and $t \approx 1800$ fs in *Fig. 4(b)*. This is due to the electron being rapidly decelerated and re-accelerated when it is moving from the accelerating phase to the decelerating phase, then back to the accelerating phase. Since the electron's velocity v_z remains slightly less than the speed of light, c, phase slippage occurs. This causes a sudden deceleration of the electron when it starts to experience the opposite $\mathbf{v} \times \mathbf{B}$ and E_z forces. The abrupt deceleration of the electron will cause it to emit photons so strongly that the RR force can modify the electron dynamics. After the

electron slips back to the acceleration phase again, it is rapidly accelerated to tens of GeV energy in a very short amount of time. Thus, the RR effect shows up during such rapid deceleration and acceleration as seen in *Fig. 4(b)*.

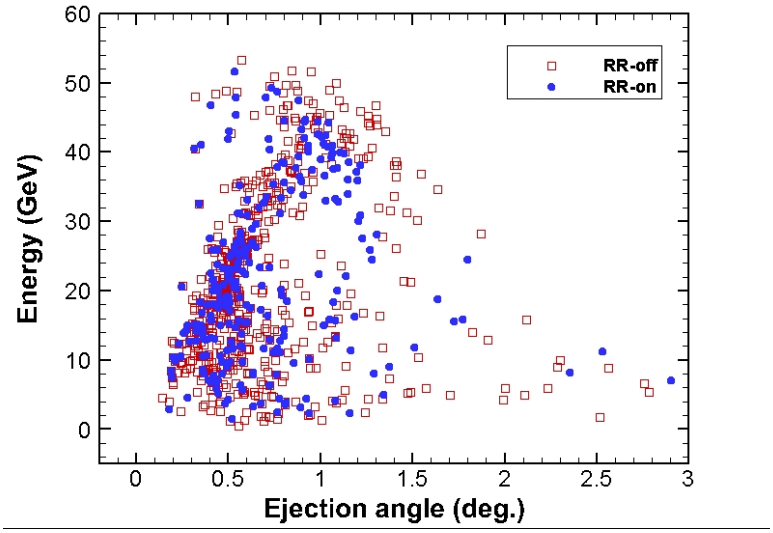

Figure 5: Monte Carlo simulation results for highly charged ions interacting with a 10^{25} W/cm^2 intensity laser pulse. The final energies of the ionized electrons are plotted as a function of the ejection angle. The laser parameters are the same as those in *Fig. 3(b)*. The highly charged ions are assumed to be at rest initially and to be distributed randomly within a cylindrical volume (having a radius of 10 μm and a length of 4 μm) that is oriented along the *z* axis and centered about the laser focusing point.

To see the RR effect on macroscopic samples, we conducted simulations for ensembles of electron trajectories at the laser intensity of 10^{25} W/cm^2. The highly charged ions were randomly given positions on the *x*-*y* plane with a radius of 10 μm, and positions on the *z* axis in the range of [-2 μm, 2 μm] around the focus center at $z = 0$. The ensemble simulation results are presented in *Fig. 5*. We define the angle $\theta = \cos^{-1}\left(\frac{p_z}{|\boldsymbol{p}|}\right)$ as the electron ejection angle between the electron ejection direction and the laser propagation direction where p_z and $\mathbf{p}$ are the *z* component and total momentum at the end of the electron trajectory, respectively. The final kinetic energies of the ionized electrons are $E = (\gamma - 1)m_e c^2$. *Fig. 5* shows that in order for the

electrons to reach high energies, their ejection angles must be small, since a smaller ejection angle indicates a longer path in the laser focusing area. The electrons are not heavily scattered as a result of the small RR force and therefore the electrons remain highly energized even when RR is turned on. Our results show that despite the large amounts of electron acceleration in the highly charged ion scenario, the RR force (which is dependent on the magnitude of the particle acceleration) is insignificant even at a laser intensity of 10^{25} W/cm^2. *Figs. 3 and 4* show that the force has little effect on the electron trajectory and consequently allows the electron to remain in the laser focusing area for an extended period of time similar to when RR is off.

B. Electron pulse

The electron pulse scenario shows very different results from the highly charged ion scenario. In this section, we consider the interaction between a laser pulse with the previously provided parameters and a 1-GeV electron pulse counter-propagating with respect to the laser pulse. Our simulations with and without radiation reaction show that the RR force causes the electrons to scatter and lose significant amounts of energy at laser intensities at and below 10^{23} W/cm^2. At a laser intensity of 10^{24} W/cm^2, however, large numbers of electrons actually reverse their momentum and are then occasionally re-accelerated by the laser pulse.

We first conducted single-trajectory simulations with and without the radiation reaction force. For single trajectory simulations, the electron was assumed to move along the negative *z* axis. The initial position and momentum of the electron were as previously calculated in **Sec. II**. The parameter of z_0 was chosen so that the electron meets the laser peak at the center of focus.

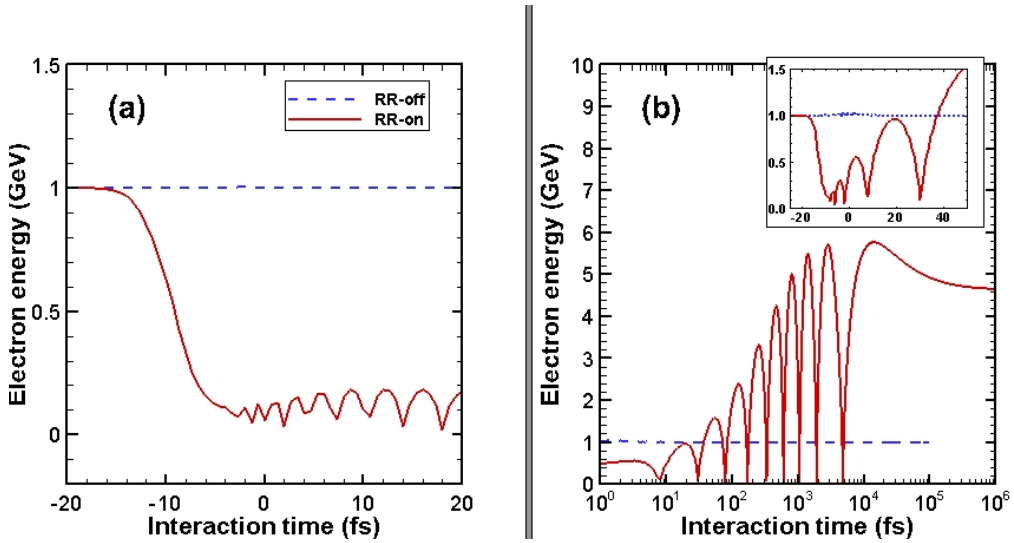

Figure 6: Monte Carlo simulation results for a single 1-GeV counter-propagating electron pulse interacting with a super-intense laser. (a) The energy in GeV of the electron pulse interacting with a 10^{23} W/cm^2 laser is plotted as a function of time in fs. (b) The same plot is shown except that the electron pulse is interacting with a 10^{24} W/cm^2 laser pulse. The inset graph shows the electron's energy before and immediately after the peak of the laser pulse. The laser parameters are the same as those in *Fig. 3*.

In *Fig. 6(a)*, the graph shows that when RR is turned off at a laser intensity of 10^{23} W/cm^2, the electron pulse simply passes through the laser pulse gaining and then losing insignificant amounts of energy, resulting in a final electron energy of 1 GeV. When RR is turned on, the electron experiences severe energy loss as it nears the peak of the laser pulse at time = 0 fs. The laser force acting against the electron results in great deceleration. This deceleration generates large amounts of emitted radiation, causing the electron to lose almost all of its initial energy. Therefore, this scenario effectively converts the electron pulse's kinetic energy into radiation. The oscillation after the energy loss is due to the particle continuing to experience the counter-propagating laser field.

A different result is found when the electron pulse interacts with a laser pulse of intensity 10^{24} W/cm^2. We see in *Fig. 6(b)* that when RR is off, the electron behaves in the same way as when interacting with a laser pulse of intensity 10^{23} W/cm^2. When RR is on, the electron first

loses its energy; later on, the electron is accelerated by the laser pulse to GeV energies. As the electron pulse counter-propagates with respect to the laser pulse, two forces act on it: the laser force and the RR force. At a laser intensity of 10^{24} W/cm^2, the laser force is greater than at 10^{23} W/cm^2. This greater laser force also causes a greater RR force as seen in *Eq.* 2. With both forces acting against the momentum of the electron pulse, the electron pulse is turned around by these forces and co-propagates with respect to the original laser pulse. The electron pulse is thus re-accelerated by the laser pulse and gains significant amounts of energy before exiting the laser focus region.

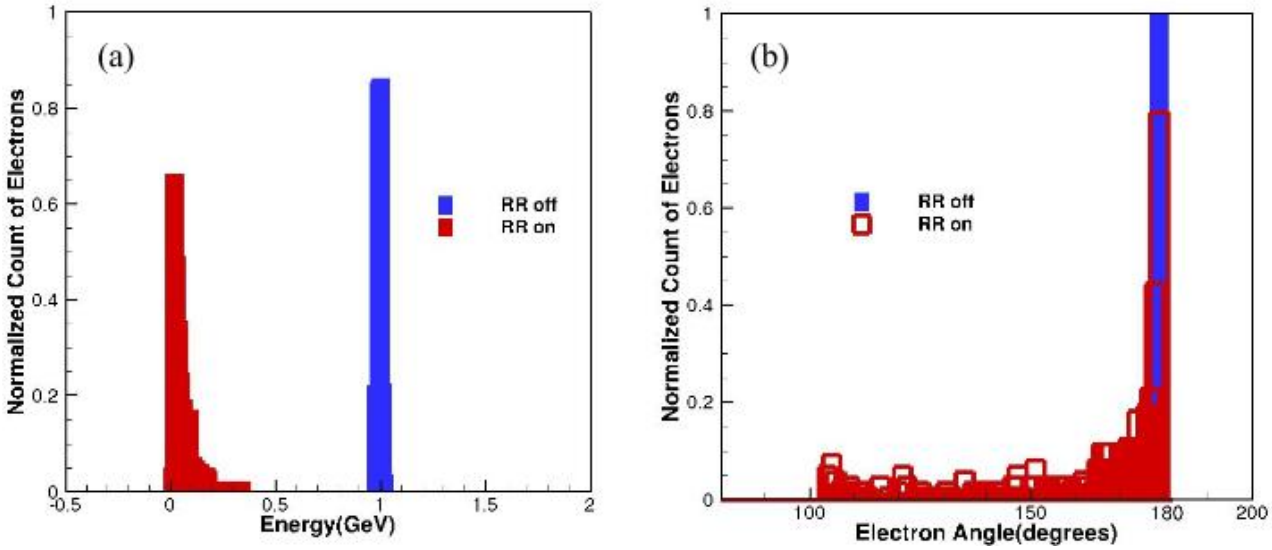

Figure 7: Monte Carlo simulation results for 1-GeV counter-propagating electron pulses interacting with a 10^{23} W/cm^2 intensity laser pulse. (a) The normalized distribution of final electron energies, which shows that with RR, all electrons exit the focusing area with less than 0.5 GeV of energy. (b) The normalized distribution of final electron angles (relative to the *z* axis), which shows that with RR, most electrons are scattered by the laser pulse. The laser parameters are the same as those in *Fig. 3*. The electrons are distributed randomly within a cylindrical volume (having a radius of 10 μm and a length of 4 μm) that is oriented along the *z* axis.

Finally, we conducted simulations for ensembles of electron trajectories at the laser intensities 10^{23} and 10^{24} W/cm^2. The electron pulses were randomly given positions on the *x* and *y* axes within a radius of 10 μm, and positions on the *z* axis in the range of $[z_0 - 2\ \mu\text{m}, z_0 + 2\ \mu\text{m}]$ from the originally calculated position z_0. The momentum of each electron in the electron pulse was randomly chosen from a normally distributed sample previously explained in **Sec. II**. We present the sample simulation results as bar graphs in *Fig. 7* for the case of 10^{23} W/cm^2. The plot supports our results from the single trajectory simulations at 10^{23} W/cm^2. Without RR, the blue bars in *Fig. 7* show that the final electron energy equals the initial 1 GeV energy, and the electrons still propagate towards the negative *z* axis ($\theta=180^o$ relative to the laser propagation direction). These results show that the electron pulses leave the laser focus region virtually unaffected by the laser pulse. When RR is turned on, the red bars in *Fig. 7* show that the electrons lose more than half of their initial energy and that they are scattered. The wide range of electron angles in *Fig. 7(b)* is caused by the RR force which, when strong enough, pushes the electrons out of the laser focusing region. A significant number of electron trajectories with RR result in a final electron angle of 180º, which means that the electrons were not scattered in that situation. This is likely due to the variation in the initial momentum and the transverse placement of electrons.

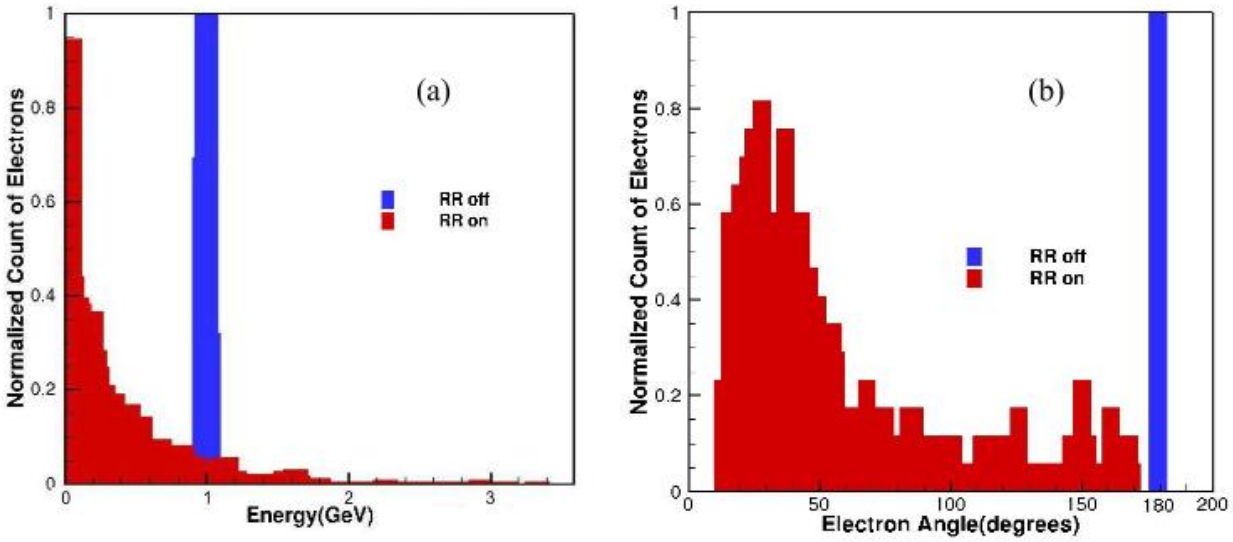

Figure 8: Monte Carlo simulation results for 1-GeV counter-propagating electron pulses interacting with a 10^{24} W/cm^2 intensity laser pulse. (a) The normalized distribution of final electron energies. (b) The normalized distribution of final electron angles, which shows that most electrons are scattered by the laser pulse. The laser parameters are the same as those in *Fig. 3*. The electron pulses are distributed in the same way as described in *Fig. 7*.

In contrast to the electron pulse interactions shown in *Fig. 7*, *Fig. 8* depicts that at a laser intensity of 10^{24} W/cm^2, the majority of electrons have final electron angles less than 90º [see *Fig. 8(b)*]. This shows that the electrons are being turned around by the laser field and radiation reaction force. The electrons now either lose most of their energy after being scattered in the positive or negative *z* direction, or gain back energy from the laser field while being re-accelerated, similar to the results graphed in *Fig. 6(b)*. This energy gain can be quite significant with final energies occasionally over 3 GeV. Most of the electrons turned around for acceleration never reach high energies, however, and leave the focus region at around ~50 degrees in the positive *z* direction.

Our results show that the RR effect causes the electron pulse to release large amounts of radiation. Without RR on, the electron pulse simply passes through the laser pulse with little effects. When RR is on, however, the electron trajectories are significantly altered. At a laser

intensity of 10^{23} W/cm^2, the electrons scatter due to the laser pulse and lose more than half of their initial energy to emitted radiation. When we increase the laser intensity to 10^{24} W/cm^2, some of the electrons continue to behave as seen when interacting with 10^{23} W/cm^2 lasers. However, most of the electrons are turned around by the combination of the laser force and the RR force to co-propagate with the laser pulse. While most electrons are scattered out of the focus region before getting accelerated to high energies, some of the co-propagating electron pulses go on to be re-accelerated by the laser pulse to GeV energies. The electron pulse scenario would be an effective method for generating radiation and if harnessed, this radiation could potentially be applied in other fields of research.

IV. Summary and Conclusions

In this paper, the relativistic classical trajectory Monte Carlo method has been used to simulate the interactions of electrons ionized from highly charged ions and electron pulses with ultra-intense laser pulses. In the highly charged ion scenario, we simulated the acceleration of electrons ionized from hydrogen-like highly charged ions interacting with an intense, tightly focused laser field. We also considered the interaction of a 1-GeV electron pulse counter-propagating with respect to the super-intense laser pulse. In the highly charged ion scenario, it is found that the radiation reaction force does not have a great effect on the electron trajectories after ionization even at a laser intensity of 10^{25} W/cm^2. For the case of laser pulse "collisions" with electron pulses, the radiation reaction force significantly alters the electron trajectories. At a laser intensity of 10^{23} W/cm^2, the electrons lose significant amounts of energy and are scattered as a result of the radiation reaction force. When the intensity is increased to 10^{24} W/cm^2, the electrons are either scattered or turned around to co-propagate with the laser pulse. Most

electrons that are turned around are scattered out of the focus region before reaching high energies, while a few electrons are re-accelerated by the laser pulse to GeV energies.

Acknowledgements

This project owes much thanks to Dr. Hu who was always ready to give feedback and support no matter how small or large the difficulty. I would also like to thank Dr. Craxton for his suggestions and for the opportunity to be a part of this program, and Dr. Enck for his unwavering encouragement the past few years. Finally, I thank the Laboratory for Laser Energetics for providing resources and granting an invaluable research experience.

References

[1] V. Yanovsky, V. Chvykov, G. Kalinchenko, P. Rousseau, T. Planchon, T. Matsuoka, A. Maksimchuk, J. Nees, G. Cheriaux, G. Mourou, and K. Krushelnick, Opt. Express **16**, 2109 (2008)

[2] T. Tajima and G. Mourou, Phys. Rev. ST Accel. Beams **5**, 031301 (2002)

[3] F. V. Hartemann, S. N. Fochs, G. P. Le Sage, N. C. Luhmann, Jr., J. G. Woodworth, M. D. Perry, and Y. J. Chen, and A. K. Kerman, Phys. Rev. E **60**, 7473 (1999)

[4] C. H. Keitel, J. Phys. B **29**, L873 (1996)

[5] S. X. Hu, and A. F. Starace, Phys. Rev. Lett. **88**, 245003 (2002)

[6] S. X. Hu, and A. F. Starace, Phys. Rev. E **73**, 066502 (2006)

[7] L. D. Landau and E. M. Lifshitz, in *The Classical Theory of Fields*, 3rd Ed. (Pergamon Press, Oxford, 1971), Vol. 2, Chap. 7, p. 208.

[8] I. N. Ross, J. L. Collier, P. Matousek, C. N. Danson, D. Neely, R. M. Allott, D. A. Pepler, C. Hernandez-Gomez, and K. Osvay, Appl. Opt. **39**, 2422-2427 (2000)